Materials Research Express

PAPER

Significant role of antiferromagnetic $GdFeO_3$ on multiferroism of bilayer thin films

RECEIVED
19 December 2017

REVISED
16 January 2018

ACCEPTED FOR PUBLICATION
30 January 2018

PUBLISHED
28 February 2018

Jyoti Shah[1], **Priyanka Bhatt**[2], **K Diana Diana Dayas**[1,3] **and R K Kotnala**[1]

[1] CSIR-National Physical Laboratory, Dr K S Krishnan Road, New Delhi-110012, India
[2] Department of Physics, Graphic Era University, Dehradun-248002, India
[3] AcSIR-National Physical Laboratory, Dr K S Krishnan Road, New Delhi-110012, India

E-mail: shah.jyoti1@gmail.com

Keywords: bilayer film, pulsed laser deposition, antiferromagnetic $GdFeO_3$, magnetoelectric coupling, strained film

Abstract

Inversion of $BaTiO_3$ and $GdFeO_3$ thin films in bilayer configuration has been deposited by pulsed laser deposition technique. A significant effect of strain on thin film has been observed by X-ray diffraction analysis. Tensile strain of 1.04% and 0.23% has been calculated by X-ray diffraction results. Higher polarization value 70.4 $\mu C\ cm^{-2}$ has been observed by strained $BaTiO_3$ film in $GdFeO_3/BaTiO_3$ bilayer film. Strained $GdFeO_3$ film in $BaTiO_3/GdFeO_3$ bilayer configuration exhibited ferromagnetic behaviour showed maximum magnetization value of 50 emu gm^{-1}. Magnetoelectric coupling coefficient of bilayer films have been carried out by dynamic method. Room temperature magneto-electric coupling 2500 mV cm^{-1}-Oe has been obtained for $BaTiO_3/GdFeO_3$ bilayer film. The high ME coupling of the $BaTiO_3/GdFeO_3$ bilayer film reveals strong interfacial coupling between ferroelectric and ferromagnetic dipoles. On magnetoelectric coupling coefficient effect of ferromagnetic $GdFeO_3$ layer has a significant role. Such high value of ME coupling may be useful in realization of magnetoelectric RAM (MeRAM) application.

Introduction

Over the past decade, a significant research progress has been focused on multiferroic thin film heterostructures. Mostly strong interfacial strain mediated magnetoelectric coupling has been reported in multilayerd multiferroic thin films [1–4]. In recent years, giant magnetoelectric coupling has been reported in multi-layered multiferroic thin films [5, 6]. Giant magnetoelectric coupling may fulfill the realization of magnetoelectric RAM (MeRAM) concept. In MeRAM, magnetization can be controlled by applying voltage which consumes low power/less energy than existing operated MRAM. Until now, a significant role of antiferromagnetic $BiFeO_3$(BFO) thin film has been observed in high magnetoelectric coupling in bilayer and multilayerd $BiFeO_3/BaTiO_3$ thin films [7, 8]. However, the critical issues, such as low electrical resistivity and weak ferromagnetic ordering, are still need to be conquered in BFO [9–13]. Breaking of space and time inversion symmetry in antiferromagnetic Cr_2O_3ompound displays unusual multiferroic effects. Spin driven ferroelectricity has been explored in antiferromagnetic rare earth orthoferrites. Room temperature multiferrocity in $SmfeO_3$ has been reported due to inverse D-M interaction between Fe spins [14]. Rare earth ferrite such as $GdFeO_3$ has been studied for many decades due to its interesting magnetic, optic, and sensing properties. The structure of $GdFeO_3$ has been derived from cubic perovskite, where the six-coordinated iron octahedra have been slightly tilted, lowering the symmetry to orthorhombic. $GdFeO_3$ has been studied for its opto-magnetic properties, gas sensing capability, and has been considered for application in bubble-domain memory devices [15]. In $GdFeO_3$ (GFO), spin exchange striction between Gd and Fe resulted into ferroelectricity near 2.5 K and exhibited magnetoelectric coupling [16]. Such strong spin mediated exchange striction in rare earth ferrate might have remarkable effect at interface with ferroelectric thin film. Very few literatures on rare earth orthoferrite and $BaTiO_3$ (BTO) multilayers have been explored for magnetoelectric coupling [17]. In present paper effect of inversion of ferroelectric BTO and antiferromagnetic GFO thin film in

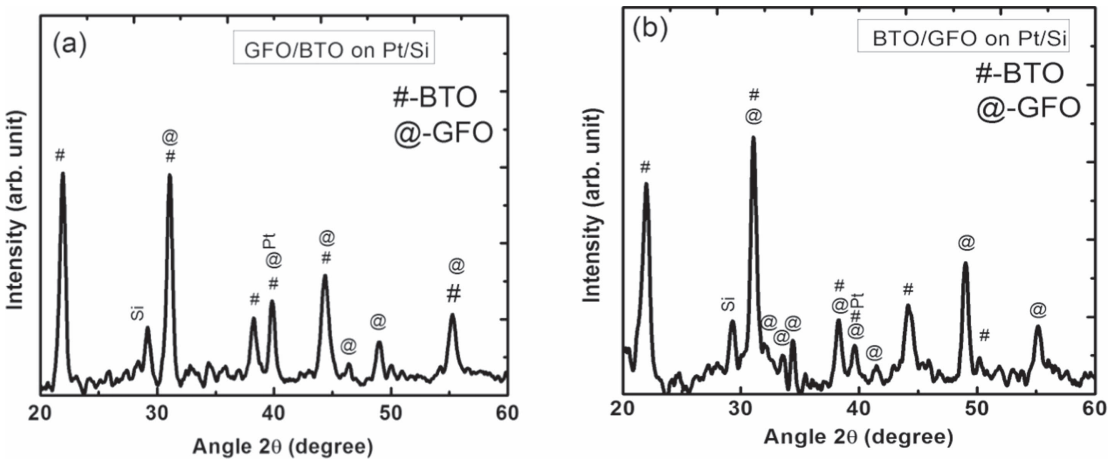

Figure 1. XRD of polycrystalline thin film (a) bilayer thin film of GFO/BTO, (b) BTO/GFO bilayer film.

bilayer configuration has been studied. Crystal structure, magnetic, ferroelectric and magnetoelectric coupling studies are undertaken in $GdFeO_3/BaTiO_3$ (GFO/BTO) and $BaTiO_3/GdFeO_3$ (BTO/GFO) bilayer thin films. A significant role of crystalline structure of antiferromagnetic GFO has been obtained in BTO/GFO/Pt/Si bilayer thin film.

Experimental

Bilayer GFO/BTO and BTO/GFO thin films were deposited on Pt/Si (111) substrate by pulse laser deposition (PLD) using KrF excimer laser ($\lambda = 248$ nm). One inch circular targets of $GdFeO_3$ and $BaTiO_3$ have been synthesised by conventional solid state method. Base pressure of PLD chamber was achieved to 6.0×10^{-6} torr before executing film deposition. Initially BTO has been deposited on Pt/Si (111) followed by GFO while substrate temperature kept at 700 °C for GFO/BTO bilayer film. Inverse deposition were executed for BTO/GFO film at optimized growth rates 0.55 Å sec^{-1}. Deposition was carried out at oxygen pressure 3×10^{-3} torr in PLD chamber. After deposition films were annealed at 500 °C in furnace for crystallization. The total thickness of $BaTiO_3/GdFeO_3$ and $GdFeO_3/BaTiO_3$ were measured approximately 200 nm by using probe station. Circular platinum top electrodes of 0.5 mm dia. were sputtered using mask on these bilayers to investigate electrical properties of thin films. The crystalline phases and structure of the films were determined by X-ray diffractometer Rikagu Ultima V with Cu-Kα ($\lambda = 0.154$ nm) radiation. Magnetic measurements were carried out by vibrating sample magnetometer (VSM, Lakeshore 7304). Ferroelectric measurements were performed using a PE loop tracer. Magneto electric measurement was done by an in-house build set up of dynamic method.

Results and discussion

Structural analysis by X-ray diffraction

Crystalline phase of bilayer thin films of GFO/BTO and BTO/GFO has been investigated by X-ray diffraction pattern in θ–2θ scan shown in figures 1(a), (b) respectively. Diffraction peaks of polycrystalline BTO and GFO have been appeared in XRD pattern which confirms crystalline nature of films. Furthermore, high intensity peaks in GFO/BTO bilayer thin film appears around $2\theta = 21.79, 30.19, 36.85, 44.42$ corresponds to planes (001), (101), (111), (002) respectively corresponding to BTO, indicating tetragonal structure and few low intensity peaks of GFO are also present, shown in figure 1(b). In BTO/GFO bilayer thin film, figure 1(b) depicts dominant XRD peaks of Pnma space group of GFO pervoskite structure. Diffraction pattern of both films reveal sandwiched layer has shown good crystallinity than top layer. Bilayer BTO/GFO film is expected to exhibit good magnetic character and GFO/BTO film to have high polarization value. BTO and GFO films have been deposited on Pt thin film exhibits strain in their crystalline structure due to lattice mismatch. Strain modulus developed in sandwiched film has been calculated using equation $s = 1a_f - a_b1 \times 100/a_b$ [18], where a_f and a_b are the lattice constants for thin film and bulk compound. Lattice constant values of BTO and GFO thin film has been calculated by X-ray diffraction pattern. Bulk lattice constant values for BTO and GFO are compared with standard JCPDS cards and provided in table 1 [18]. The value of strain (%) for sandwiched BTO and GFO films in bilayer thin film were calculated 1.04% and 0.24% respectively. For upper BTO and GFO layers in bilayer

Table 1. Strain values calculated for BTO and GFO lattices in bilayer thin films.

Lattice parameter (BTO)			Strain	Lattice parameter (GFO)			Strain
	a (A°)	c (A°)	(%)	a (A°)	b (A°)	c (A°)	(%)
Bulk value	3.999	4.0335	compressive	5.616	7.669	5.346	compressive
Upper layer thin film	3.994	4.334	0.023(almost relaxed)	5.597	7.651	5.350	0.11(almost relaxed)
Sandwiched layer thin film	4.300	4.075	1.04 (tensile)	5.555	7.511	5.333	0.24 (tensile)

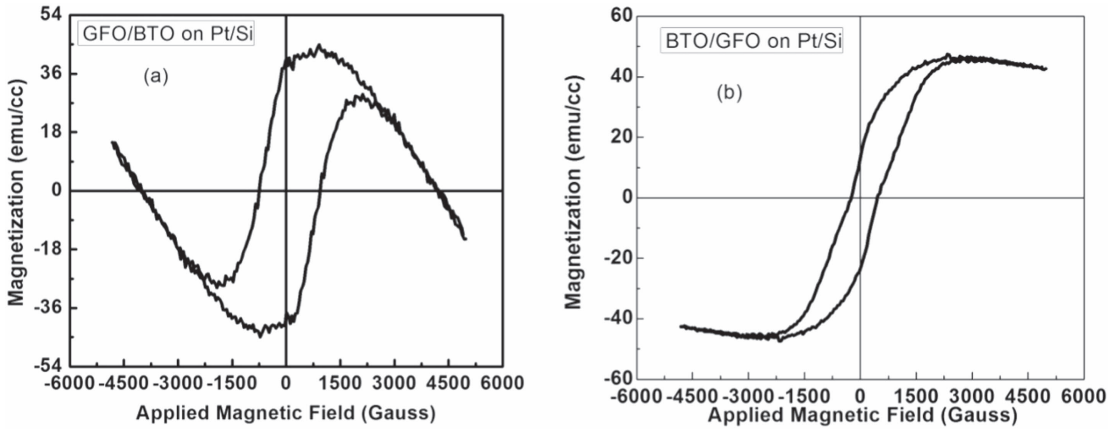

Figure 2. Magnetic hysteresis loop of (a) weak ferromagnetic hysteresis loop of GFO/BTO and (b) ferromagnetic hysteresis loop of BTO/GFO bilayer thin film.

films resulted in 0.023% and 0.11% strain respectively. $LuFeO_3$ also exhibits an orthorhombic $GdFeO_3$-type structure exhibited strain 0.39% applied by the substrate [18]. For $GdFeO_3$ sample, the diffraction peaks are slightly shifted towards higher 2θ values compared with the bulk material. Possibly due to strain volume of the unit cell decreases from bulk material [15]. A large value of strain present in BTO in GFO/BTO thin film indicates a large lattice distortion which may lead to improved ferroelectric property.

Magnetization measurement

Magnetic hysteresis loops of bilayer thin films have been plotted after subtracting the substrate and buffer layers, hysteresis contributions as shown in figures 2(a), (b). Bilayer GFO/BTO film shows weak ferromagnetism at low magnetic field 1500 Oe in MH loop in figure 2(a). On increasing applied magnetic field diamagnetic behavior of BTO dominated. Bilayer BTO/GFO film MH loop figure 2(b) shows ferromagnetic behavior. In $GdFeO_3$ magnetic field along the *c*-axis can induce not only a weak ferromagnetic moment, but also a ferroelectric polarization [19]. Interfacial strain induces magnetization in antiferromagnetic GFO. Antiferromagnetism in GFO arise due to antiferromagnetic exchange interaction between Fe^{3+} ions via oxygen ion. Ferromagnetism arises due to imbalance spin magnetic moment in GFO structure that could be generated due to strain developed in structure. The anti-symmetric super exchange interaction of Fe ions due to strain results in tilting of spins and hence ferromagnetism is observed. MH loop shows saturation magnetization of 50 emu/cc in BTO/GFO film. It signifies strain developed in crystalline structure of GFO resulted into unequal magnitude of antiferromagnetic domains. The exchange coupling at bilayer interface of BTO/GFO has been also observed in MH loop with slight compressed loop at centre. It reveals at interface, strained GFO spins has exchange coupling with BTO surface spins that pins the magnetic movement at low applied field.

Polarization measurements

Ferroelectric behavior of bilayer thin films of GFO/BTO and BTO/GFO taken by platinum top and bottom electrodes by PE loop measurement shown in figures 3(a), (b). Bilayer thin film of GFO/BTO showed polarization of 70.4 $\mu C\ cm^{-2}$ at applied electric field 6 kV cm^{-1} and high value of remnant polarization, 48 $\mu C\ cm^{-2}$. It has been confirmed by XRD the crystalline nature of BTO in GFO/BTO film. High value of saturation polarization may be due to strain developed in sandwiched layer of BTO leads to distortion in unit cell. Tensile strain developed in sandwiched BTO layer has been obtained 1.0% by XRD exhibited higher polarization value [20]. Such strain effect on polarization has been also found in CFO-PZT bilayer thin film [21]. A spontaneous polarization has been observed up to 0.12 $\mu C\ cm^{-2}$ in $GdFeO_3$ below the antiferromagnetic ordering temperature of Gd^{3+} (2.5 K), without an assistance of magnetic field [22]. BTO/GFO bilayer exhibited

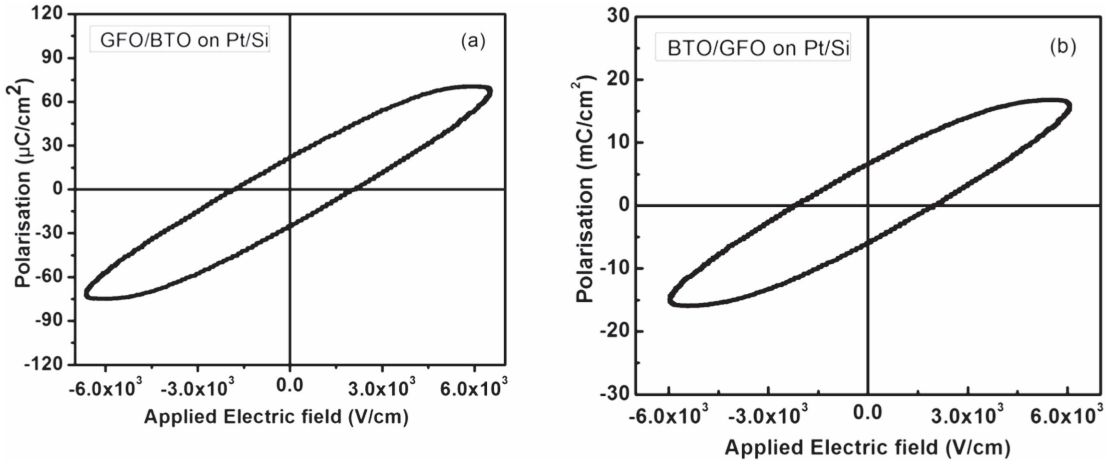

Figure 3. Polarization hysteresis loop (a) bilayer film GFO/BTO (b) bilayer film BTO/GFO at room temperature.

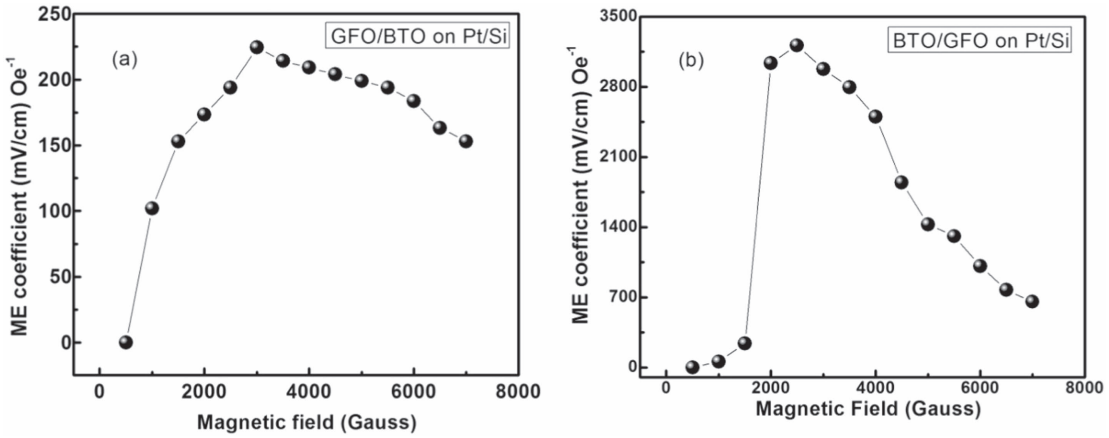

Figure 4. Magnetic field dependence of magneto- electric coupling coefficient in longitudinal direction of (a) bilayer film GFO/BTO (b) bilayer film BTO/GFO.

16.6 μC cm^{-2} saturation polarization may be due relaxed top BTO layer. $LuFeO_3$ exhibited ferroelectric polarization due to non-collinear spin structure showed a canted antiferromagnetic order, leading to a strong coupling between magnetization and polarization at room temperature [23]. Lower remnant polarization 12 μC cm^{-2} obtained for BTO/GFO relaxed top BTO film [24]. Corrosive field 2Ec of GFO/BTO found to be 3.9 kV cm^{-1} while that of BTO/GFO was 4.2 kV cm^{-1}. Higher value of corrosive field in BTO/GFO may be due to exchange interaction effect between BTO and GFO film interface as observed by compressed MH loop. Polarization values suggested strained crystalline structure confirmed by XRD has a significant role in ferroelectricity in GFO/BTO film.

Magnetoelectric coupling of bilayer interface

Magnetoelectric coupling measurement of two bilayer thin films has been taken by using dynamic method with in-house build set up shown in figures 4(a), (b) [25]. Room temperature ME measurement has been carried out at 1 Oe, 999 Hz AC field and DC magnetic field (Ho) was applied collinear with AC field. DC magnetic field was applied perpendicular to the film plane and electric field developed was measured using a lock in amplifier in mV to calculate ME coupling coefficient. Film samples were poled prior to ME measurement. The value of coupling coefficient (α_{ME}) was calculated from the expression $\alpha_{ME} = \delta V/(\delta H_{ac}.t)$ where δV is the voltage developed across the sample, δH_{ac} is AC magnetic field and t is the thickness of film [26]. Magnetoelectric coupling coefficient α_{ME} has been calculated ~224.5 mV cm^{-1} Oe for GFO/BTO film at applied DC magnetic field 3000 Gauss. The ME coefficient α_{ME} for BTO/GFO has been found ~2500 mV cm^{-1} Oe at 2500 Gauss DC magnetic field shown in figure 4(b). Gigantic magnetoelectric phenomena in rare earth ferrate $DyFeO_3$ has been reported below the antiferromagnetic ordering temperature [19]. The ME coupling of the multiferroic composites mainly arises from the magnetic-mechanical-electric exchange interaction between the magnetostrictive and

ferroelectric phases through the stress/strain developed at interface [26–28]. Not only a magnetic-field-control of polarization but also an electric-field-control of magnetic moment were realized in $RFeO_3$ ($R = Dy_{0.7}Tb_{0.3}$ or $Dy_{0.75}Gd_{0.25}$) [29]. It has been found by XRD, MH and PE loop measurements of sandwiched layer that is crystalline, has a significant impact on material property. All results suggest magnetoelectric coupling is significantly dependent on magnetization of antiferromagnetic GFO layer. Gadolinium ferrite exhibit spinstriction behaviour at applied magnetic field that is exchange coupled with ferroelectric domains to rotate [30]. On further increasing applied magnetic field Fe^{3+}/Gd^{3+} spins re-orientate that leads to a sudden drop of polarization hence ME coupling [31]. The observed value of ME coupling coefficient in BTO/GFO bilayer thin film is significantly higher. Since ME coupling is a spin exchange coupling effect and is more pronounced in quantum confined dimensions thus BTO/GFO exhibited high value of ME coefficient. High α_{ME} of BTO/GFO composite film reveals strong interfacial coupling between ferroelectric and ferromagnetic dipoles.

Conclusions

Crystalline bilayer thin films of GFO/BTO and BTO/GFO have been deposited by pulsed laser deposition technique. Effect of strained crystalline phase on ferroelectric and ferromagnetic properties has been clearly observed by X-ray diffraction, polarization and magnetization measurements. Bilayer GFO/BTO film exhibited high saturation polarization value of 70.4 μC cm^{-2} due to strained BTO film. Distortion in perovskite antiferromagnetic GFO film attained saturation magnetic moment of 50 emu gm^{-1} in BTO/GFO bilayer thin film. It has been observed that interfacial strain produced in bilayer films has a significant role in polarization and magnetization. Magnetoelectric coupling coefficients of bilayer thin films of GFO/BTO and BTO/GFO have been measured by dynamic method. On magnetoelectric coupling coefficient, effect of ferromagnetic GFO layer has a dominant role. Highest ME coupling of 2500 mV-Oe/cm has been calculated for BTO/GFO bilayer thin film. Such a high value of coupling coefficient can be useful for MeRAM and transducer applications.

Acknowledgments

Authors are thankful to Director CSIR-NPL for constant support and encouragement. Author JS is thankful to Department of Science & Technology for the grant received under the scheme DISHA project DST/Disha/SoRF-PM/034/2013(G).

ORCID iDs

Jyoti Shah https://orcid.org/0000-0002-6570-4813

References

[1] Lorenz M *et al* 2014 *J. Phys. D: Appl. Phys.* **47** 135303
[2] Kulkarni A, Meurisch K, Teliban I, Jahns R, Strunskus T, Piorra A, Kn€ochel R and Faupel F 2014 *Appl. Phys. Lett.* **104** 022904
[3] Greve H, Woltermann E, Quenzer H-J, Wagner B and Quandt E 2010 *Appl. Phys. Lett.* **96** 182501
[4] Fiebig M, Lottermoser T, Meier D and Trassin M 2016 *Nat. Rev. Mater.* **1** 16046
[5] Srinivasan G, Rasmussen E T, Gallegos J, Srinivasan R, Bokhan Y I and Laletin V M 2001 *Phys. Rev.* B **64** 21440
[6] Zheng H *et al* 2004 *Science* **303** 661
[7] Gupta R, Chaudhary S and Kotnala R K 2015 *ACS Appl. Mater. Interfaces* **7** 8472
[8] Lorenz M, Hirsh D, Patzig C, Höche T, Hohenberger S, Hochmuth H, Lazenka V, Temst K and Grundmann M 2017 *ACS Appl. Mater. Interfaces* **9** 18956–65
[9] Wang Y P, Zhou L, Zhang M F, Chen X Y, Lu J M and Liu Z G 2004 *Appl. Phys. Lett.* **84** 1731–3
[10] Yang P, Kim K M, Joh Y G, Kim D H, Lee J Y, Zhu J and Lee H Y 2009 *J. Appl. Phys.* **105** 061618 4pp
[11] Lee Y H, Wu J M, Chueh Y L and Chou L J 2005 *Appl. Phys. Lett.* **87** 172901 3pp
[12] Yuan G L, Or S W, Chan H L W and Li Z G 2007 *J. Appl. Phys.* **101** 024106 4pp
[13] Li M, Hu Z, Pei L, Liu J, Wang J, Yu B and Zhao X 2011 *Ferroelectrics* **410** 3–10
[14] Lee J-H, Jeong Y K, Park J H, Oak M-A, Jang H M, Son J Y and Scott J F 2011 *Physical Review Letter* **107** 117201–5
[15] So¨derlind F, Selegad L, Nordblad P, Uvdal K and Ka¨ll P-O 2009 *J Sol-Gel SciTechnol* **49** 253–9
[16] Tokunaga1 Y, Furukawa N, Sakai H, Taguchi Y, Arim T-H and Tokura Y 2009 *Nature Materials* **8** 558–62
[17] Zhao H, Peng X, Zhang L, Chen J, Yan W and Xing X 2013 *Applied Physics Letters* **103** 082904
[18] Sharma S, Tomar M, Kumar A, Puri N K and Gupta V 2015 *Journal of Applied Physics* **118** 074103
[19] Tokunaga Y, Iguchi S, Arima T and Tokura Y 2008 *Phys. Rev. Lett.* **101** 097205
[20] Choi K J *et al* 2004 *Science* **306** 1005
[21] Li Z, Gao Y, Yang B, Lin Y, Yu R and Nan C-W 2011 *J. Am. Ceram. Soc.* **94** 1060–6
[22] Tokunaga Y, Furukawa N, Sakai H, Taguchi Y, Arima T and Tokura Y 2009 *Nature Mater.* **8** 558–62
[23] Chowdhury U, Goswami S, Bhattacharya D, Ghosh J, Basu S and Neogi S 2014 *Appl. Phys. Lett.* **105** 052911
[24] Yang Y, Wang Z, Li J F and Viehland D 2010 *Journal of Nanomaterials* **756319** 1–5

[25] Duong G V, Groessinger R, Schoenhart M and Basques D B 2007 *J. Magn. Magn. Mater.* **316** 390–3
[26] Gupta R, Shah J, Chaudhary S and Kotnala R K 2015 *Journal of Alloys and Compounds* **638** 115–20
[27] Guo K, Zhang R, Mou Q, Cui R and Deng C 2016 *Nano Research Letters* **11** 387
[28] William R V, Marikani A and Madhavan D 2016 *J Eur Ceram Soc* **42** 6807–16
[29] Tokunaga Y, Taguchi Y, Arima T and Tokura Y 2012 *Nature Phys.* **8** 838–44
[30] Shah J and Kotnala R K 2012 *Scripta Materialia* **67** 316–9
[31] Dong S, Liu J-M, Cheong S-W and Ren Z 2015 *Advances in Physics* **64** 519–626